ACS APPLIED MATERIALS & INTERFACES

Energy, Environmental, and Catalysis Applications

Amorphous Flowerlike Goethite FeOOH Hierarchical Supraparticles: Superior Capability for Catalytic Hydrogenation of Nitroaromatics in Water

Yongjian Ai, Lei Liu, Cheng Zhang, Li Qi, Mengqi He, Zhe Liang, Hong-bin Sun, Guoan Luo, and Qionglin Liang

ACS Appl. Mater. Interfaces, **Just Accepted Manuscript** • DOI: 10.1021/acsami.8b10711 • Publication Date (Web): 04 Sep 2018

ACS Publications

is published by the American Chemical Society. 1155 Sixteenth Street N.W., Washington, DC 20036

Amorphous Flowerlike Goethite FeOOH Hierarchical Supraparticles: Superior Capability for Catalytic Hydrogenation of Nitroaromatics in Water

Yongjian Ai[a,b], Lei Liu[b], Cheng Zhang[b], Li Qi[b], Mengqi He[b], Zhe Liang[a], Hong-bin Sun[b*], Guoan Luo[c], Qionglin Liang[a*]

[a]Key Laboratory of Bioorganic Phosphorus Chemistry & Chemical Biology (Ministry of Education), Beijing Key Lab of Microanalytical Methods & Instrumentation, Department of Chemistry, Tsinghua University, Beijing 100084, P.R. China.

[b]Department of Chemistry, Northeastern University, Shenyang 110819, P.R. China.

[c]State Key Laboratory of Quality Research in Chinese Medicine, Macau Institute for Applied Research in Medicine and Health, Macau University of Science and Technology, Macau, China.

KEYWORDS: *α-FeOOH, amorphous, hierarchical supraparticles, heterogeneous catalysis, hydrogen transfer reaction*

ABSTRACT: Fabrication of anilines from the corresponding nitro aromatics is a hot topic both for academia and industry, however, conducting this protocol in water over noble metal free catalytic system is still a great challenge. Continuous efforts are being made on exploiting novel catalyst for this transformation. In this work, we developed a scalable method for synthesizing the uniform flowerlike amorphous α-FeOOH hierarchical supraparticles. The well-defined amorphous α-FeOOH was prepared through an environmentally benign method, which is hydrolysis of the self-assembled iron glycolate at room temperature. Compared with other iron-only catalysts, this flowerlike amorphous α-FeOOH hierarchical supraparticles catalyst exhibits the best performance in the catalytic reduction of nitro aromatics to corresponding anilines by using water as reaction solvent (TOF is 106 h^{-1} for 4-nitrophenol in water). The further results indicated that the amorphous structure, special nanostructures and adsorption-desorption synergy offered the excellent activity. The kinetics study shows that the reduction of 4-nitrophenol is first-order for α-FeOOH and the apparent active energy E_a is 75.9 kJ·mol^{-1}. Furthermore, this catalyst can be used for 8 times without obvious catalytic activity losing. We believe that this novel flowerlike amorphous α-FeOOH hierarchical supraparticles catalyst is a milestone in the reduction of nitro-compounds.

INTRODUCTION

Nanotechnology is changing the world. In the field of catalysis, the development of nanoscience and nanotechnology give the scientists deep views in the microstructure of the catalysts.[1–2] The fine information of these tiny particles helps us to discover new ideas to improve the efficiency of various catalysts. Some classical catalytic systems have been awakened for their new spring because the newly raised gracious structures have shown specific physical and chemical properties. For example, three-dimensional (3D) hierarchical microparticles have been widely synthesized and characterized with the development of nanotechnology.[3–7] They have attracted much attention because of their unique properties and potential applications.[8–9] Assembling well-ordered nanosheets, nanotubes or nanoribbons under the conditions of strongly anisotropic interactions leads the specific structures thus improves the mechanical properties of composite materials,[10–14] and both of the advantages of individual nanoparticles and bulk samples were integrated. The self-assemblage provides a simple and low-cost method as a controllable manner, so the assembling of individual inorganic nanoparticles into larger or microscale structures is one of the most challenging frontiers in modern materials science. [15–16]

In the past decades, iron-based catalysts have been well developed, because of its abundance, eco-friendliness, inexpensiveness and non-toxicity.[17–22] The hydrazine-mediated reduction of nitroarenes to form anilines is an eminent application of iron-based catalysts, whose activity is better than other cheap metals.[23–29] In the early of 1980s, M. Suchy and P. Winternitz reported that $FeCl_3$/C had acceptable activity for this reaction.[30] This method was almost immediately put into industry, because the contemporary processes required more than stoichiometric reductants, such as Fe/HCl, Na_2S and $SnCl_2$ and the residues had caused a lot of environmental problems. Although it has been applied in industry for more than 30 years for producing anilines, the efficiency of the $FeCl_3$/C system is limited, because the large amount of catalyst loading and the poor reusability have been criticized by the users.[31–33] Thus, in 1997~1999, Paul Rys's group published a series of works to illustrate the mechanism of the iron-catalyst. They proved that the surface area is the key factor for the catalyst's activity.[34–37] With the development of nanotechnology, the iron oxides catalyzed reduction of nitroarenes had been deeply viewed both in industry and academia. In the first 10 years of 21st century, nanosized Fe_3O_4 have been once regarded as the best catalyst, however, the record was quickly broken by the more active γ-Fe_2O_3 in

2013~2015.[38–44] The small particles of in-situ generated γ-Fe_2O_3 from $Fe(acac)_3$ can be more active with the help of a microwave reactor in organic solvent.[45–47] It was reported that the requirement of anilines and their derivatives is more than 4,000,000 tons per year for the world. The totally output value of these important chemical feedstocks will increase to £10.17 billion by 2020.[48–49] Following the instruction of these results, it is still a great challenge to develop highly active iron catalyst for the reduction of nitro aromatics, as well as to discover the catalytic mechanism of the iron catalysts.

In recent years, α-FeOOH has been broadly applied in many areas such as waste water treatment, drug delivery, energy storage devices and catalysis.[50–54] However, most of the previously reported structures are using tedious procedures and the materials were crystallized.[55–58] Due to the great flexibility of the amorphous catalyst, the catalytic performance of the amorphous catalyst was more superior to their crystalline counterparts.[59] It is highly desirable but challenging to develop a facile method to produce amorphous α-FeOOH with a 3D hierarchical structure**.**

Herein, we reported a facile methodology for the scalable synthesis of the flowerlike amorphous α-FeOOH hierarchical supraparticles. The amorphous α-FeOOH was fabricated through the hydrolysis of iron glycolate at room temperature (Figure 1) and it has been well characterized as to confirm the physical and chemical properties. This noble metal free material was a good candidate for the catalytic reduction of nitroaromatics in water. To the best of our knowledge, it is the most active iron-only catalyst for the hydrazine-mediated reduction of nitroarenes in water.

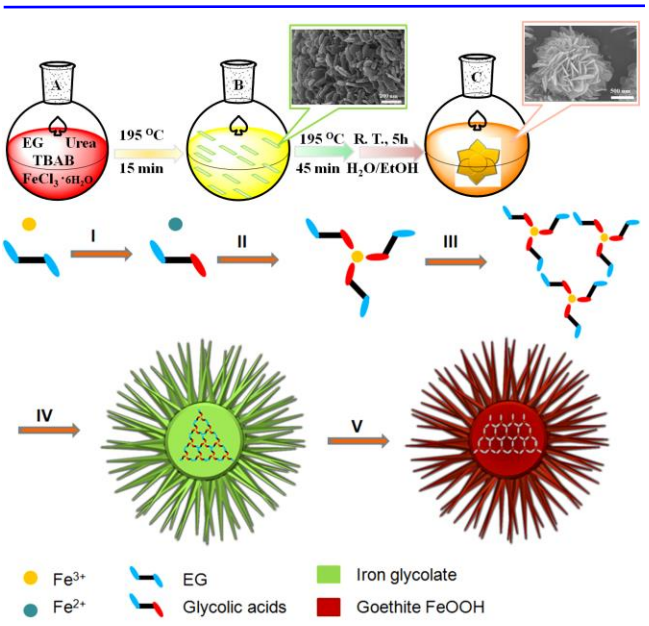

Figure 1. Schematic illustration of the morphological evolution process of the as-obtained uniform flowerlike amorphous α-FeOOH hierarchical supraparticles: (I) formation of iron glycolate nucleus; (II-III) formation of iron glycolate nucleus nanosheet; (IV) self-assemble to form the iron glycolate nanostructures; (V) hydrolysis to form the uniform flowerlike amorphous α-FeOOH hierarchical supraparticles.

EXPERIMENTS SECTION

Synthesis of iron glycolate

The iron glycolate was prepared as the following steps. Typically, 14.2 g tetrabutyl ammonium bromide (TBAB) was firstly added to 400 mL ethylene glycol (EG) in a 1000 mL round flask. As the surfactants completely dissolved, 2.4 g $FeCl_3 \cdot 6H_2O$ was added, then the solution become sanguine. After the iron ion was well dispersed, 5.4 g urea was added then the solution was ultrasonicated for 30 min. The obtained blend was moved to an oil bath and heated to 195 °C. About 15 min later, a yellow precipitate began to appear then the mixture turned into yellow-green, which indicated the formation of iron glycolate nanostructures. After refluxing for another 45 min, the mixture became completely green then the reaction was stopped and the mixture was cooled to room temperature. The green precipitate was collected by filtration under reduced pressure and washed with 1500 mL ethanol. The resulted residue was thoroughly dried overnight at 35 °C under vacuum and the obtained 1.2 g iron glycolate was kept under vacuum for further use.

Synthesis of flowerlike amorphous α-FeOOH hierarchical supraparticles

A typical experimental procedure for the synthesis of flowerlike amorphous α-FeOOH was described as follows. A portion of iron glycolate (0.6 g) was dispersed in the mixed solution of ethanol (20 mL) and deionized water (180 mL). After ultrasonication for 10 min, the green mixture solution was stirred for 5 h under ambient conditions. In this processing, the green solution turned into a brownish yellow one and the precipitate was deposited on the bottom of the round flask. The α-FeOOH was filtered under reduced pressure and washed with deionized water. The resulted residues were thoroughly dried overnight at 80 °C under vacuum and finally the flowerlike amorphous α-FeOOH hierarchical supraparticles were obtained.

Catalytic transfer hydrogenation reduction of nitroaromatics in water over the flowerlike amorphous α-FeOOH hierarchical supraparticles

In a typical procedure, 1 mmol nitroaromatics and 7 mg catalyst was added into a sealed tube, then 2 mL water was added as the solvent. After ultrasonication for 5 min, 2 mmol (125 mg, 80%) hydrazine hydrate was added. The blended solution was heated in an oil bath at the temperature of 110 °C for 60 min. The reaction process was monitored by thin layer chromatography (TLC), high performance liquid chromatography (HPLC) and gas chromatography-mass spectrometer (GC-MS). No by-product was detectable. After the reaction accomplished, the catalyst was used to the next cycle without any treatment, as to test the stability and the reusability under the same conditions. The reduction of nitroaromatics in ethanol was similar to in water except the hydrazine hydrate was 1.6 mmol (100 mg, 80%), and the reaction time was shortened to 20 min.

RESULTS AND DISCUSSION

The process for the fabrication of the flowerlike α-FeOOH

To understand the formation process of the flowerlike α-FeOOH, several samples were collected at different time during the reaction. As shown in Figure 2(a), a sample from 15 minutes-heated solution, the worm-like iron glycolate had been fabricated with a diameter of about 20 nm. By absorbing

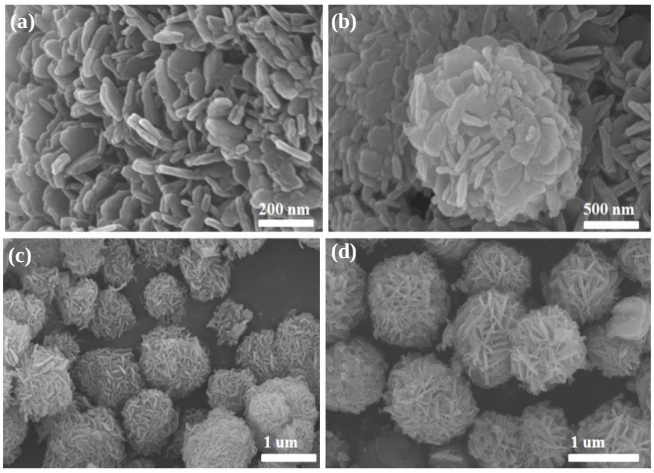

Figure 2. SEM images of the iron oxide precursors collected at different time: (a) 15 min, (b) 30 min, (c) 45 min, and (d) 60 min.

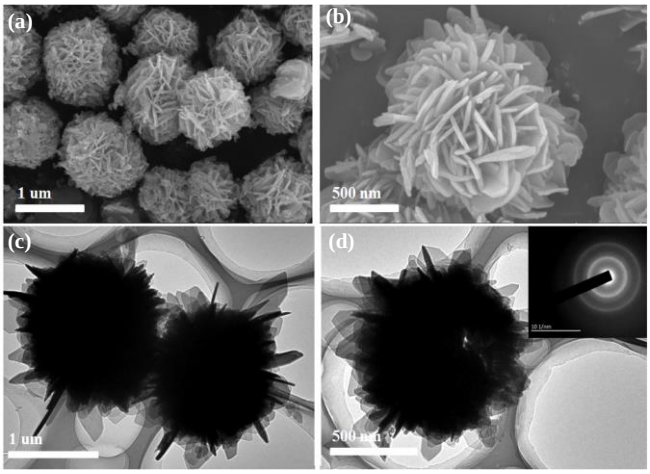

Figure 3. SEM (a-b) and HR-TEM (c-d) images of the flowerlike amorphous α-FeOOH hierarchical supraparticles.

phase transfer catalyst TBAB on certain crystal face, the embryonic nanoparticles showed anisotropy, which is the orienting initiation for the growth of nanosheet. As the reaction proceeded (Figure 2(b)), the receptacles were slowly formed with the extension of the nanosheets, and the flowerlike iron glycolate was synthesized. As time went by, the size of the iron glycolate cluster grew gradually (Figure 2(c)) by plugging more sheet. However, 1 h later, the size and morphology of the product did not change any longer (Figure 2(d)). The reason is that the self-assembling process is governed by the balance between electrostatic repulsion and Van der Waals attraction that increases as the broad polydispersity of the nanoparticles. The collected green precipitate was re-dispersed in the mixed solution of ethanol and deionized water and stirred for 5 h under air, the particles turned into brownish yellow amorphous α-FeOOH nanoflower gradually, which is a 3D hierarchical structure.

Based on the reported literatures and experimental results[51, 54], a plausible mechanism for the formation of flowerlike amorphous α-FeOOH nanostructures was illustrated as the following reactions. We speculated that the pathway included the oxidation–reduction, co-precipitation and hydrolysis reaction. As shown in reaction (1), the first step was the oxidation of EG by Fe^{3+} and to produce glycolic acids. Then the iron glycolate nuclei precursor was formed via the co-precipitation of $FeCl_3$ and glycolic acids in the presence of urea (reaction (2)). These nuclei gradually assembled into iron glycolate nanosheets. Finally, as the iron glycolate precursors were dispersed in water and exposed in air, the hydrolysis occurred and the flowerlike amorphous α-FeOOH was fabricated.

$$HOH_2C{-}CH_2OH + Fe^{3+} \xrightarrow{\text{Urea}} HOH_2C{-}COOH \quad (1)$$

$$HOH_2C{-}COOH + Fe^{3+} \xrightarrow{\text{Urea}} (HOH_2C{-}COO)_3Fe \quad (2)$$

$$(HOH_2C{-}COO)_3Fe \xrightarrow{H_2O} FeOOH + HOH_2C{-}COOH \quad (3)$$

Characterization of α-FeOOH hierarchical supraparticles

The morphology of the fabricated α-FeOOH was observed by scanning electron microscopy (SEM) and high-resolution transmission electron microscopy (HR-TEM). As shown in Figure 3 (a-b), the α-FeOOH exists as the uniform flowerlike 3D hierarchical architecture with a diameter of about 1 um.

The thickness of the subunits nanosheets was characterized by the atomic force microscope (AFM), as shown in Figure S1, it was about 5-15 nm. From the HR-TEM images (Figure 3 (c-d)), the nano-receptacles and nano-petals can be obviously observed. Furthermore, the ring-like selected area electron diffraction (SAED) pattern showed that the α-FeOOH was amorphous (Figure 3(d), inserted one).

Sometimes the formation of iron glycolate accompanies with the generation of Fe_2O_3 or Fe_3O_4 as by-products, however, our nanoflowers are pure iron glycolate according to the X-ray diffraction (XRD, Figure 4(a)). For comparison, the γ-Fe_2O_3 and Fe_3O_4 were prepared from the iron glycolate by annealing treatment (SI, Figure S2-3).[8] The purity of iron glycolate stands a good position for the further treatment to obtain pure amorphous α-FeOOH. As shown in Figure 4(a), there is no obvious characteristic diffraction peaks in the XRD pattern of the α-FeOOH nanoflower. This indicated that the obtained goethite was in amorphous state.[60] The result was greatly agreed with the SAED characterization.

We measured the specific surface area of the fabricated amorphous α-FeOOH by nitrogen adsorption-desorption analysis, the surface area was 177 $m^2\,g^{-1}$ (Figure 4(b)). The type IV isotherm was presented and the hysteresis loop indicated the existence of mesopores. The pore size distribution was calculated by BJH method from desorption branches (Figure 4(b). inserted one), and the pores of amorphous α-FeOOH were mainly in the range of 3-10 nm.

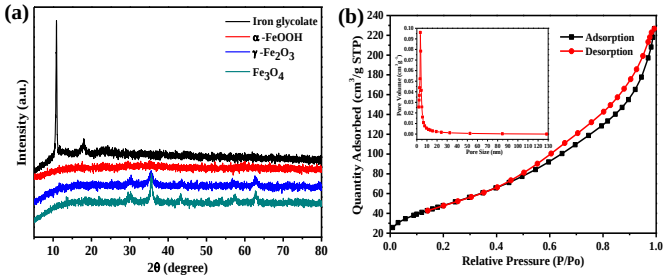

Figure 4. (a) X-ray diffraction (XRD) pattern of iron glycolate, γ-Fe_2O_3, and Fe_3O_4 and α-FeOOH; (b) nitrogen adsorption isotherms of uniform flowerlike α-FeOOH hierarchical supraparticles catalysts.

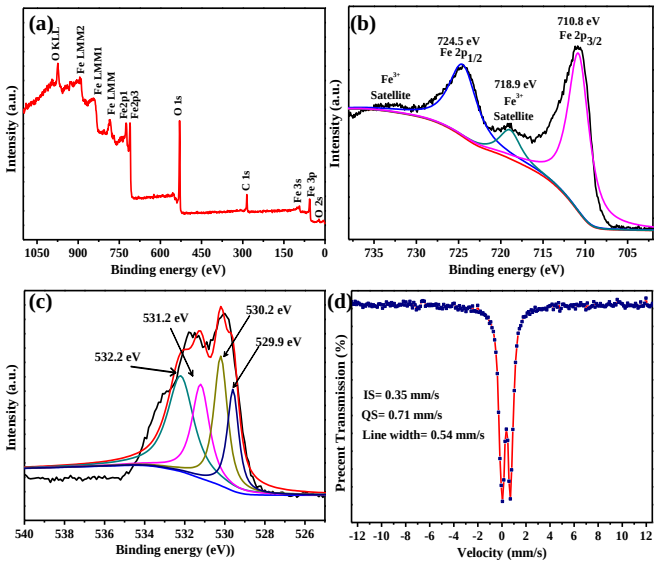

Figure 5. (a) XPS survey spectrum of the α-FeOOH; (b)XPS spectrum of the Fe 2p region; c) XPS spectrum of the O1s 2p region of the synthesized α-FeOOH supraparticles; (d) room temperature ^{57}Fe Mössbauer spectra of α-FeOOH supraparticles.

More characterization including Fourier transform infrared spectroscopy (FT-IR), Raman spectrum and X-ray photoelectron spectroscopy (XPS) were carried out to detail the chemical composition of the hydrolysis product from iron glycolate. The FT-IR spectrum of α-FeOOH hierarchical supraparticles was shown in Figure S4. The band closed to 3369 cm^{-1} was assigned to the -OH vibration. This band was a typical mode of non-stoichiometric hydroxyl units in the goethite structure. The bands centered at 1450, 979, and 648 cm^{-1} can be all identified to the Fe-O vibrational modes in α-FeOOH. The absorption band at 894 cm^{-1}, which caused by the in-plane bending of surface hydroxyl of Fe-OH-Fe, was similar to that was reported in previous literature.[61] The Raman spectroscopy (Figure S5) with bands at 243, 299, 385, 479, 550, 685, 993 and 1255cm^{-1} can be attributed to dissymmetric stretching of metal and hydroxide group, which is well agreed with the reported spectra of α-FeOOH.[62] Thermal gravimetric analysis (TGA) (Figure S6) demonstrated that as the supraparticles was calcined in air at different temperatures, the α-FeOOH rapidly transformed to the iron oxides compounds.

In order to further investigate the oxidation and existing state of iron, the XPS characterization was conducted. As shown in Figure 5(a) and Figure S7, the XPS spectrum of the α-FeOOH identified the coexistence of Fe, O elements in the sample. Furthermore, the iron atomic concentration at the surface was 10.43% (42 wt%). As shown by the XPS spectrum of the Fe 2p region (Figure 5(b)), two major peaks concentrated at 724.5 and 710.8 eV are the corresponding binding energies of Fe $2p_{1/2}$ and Fe $2p_{3/2}$, which together with two shake-up satellites (732.9 eV and 718.9 eV) indicated that the iron was remained as α-FeOOH. As Figure 5(c) shows, the XPS O 1s can be fitted by four peaks at binding energies of around 529.9, 530.2, 531.2 and 532.2 eV. These peaks were assigned to corresponding =O, -OH and chemically or physically adsorbed water respectively. These values clearly confirmed the existence of α-FeOOH.[55, 63]

The room-temperature ^{57}Fe Mössbauer spectrum was conducted to further ascertain the phase of the products, as it is sensitive to the iron-containing components. The Mössbauer spectrum of the iron glycolate (Figure S8) displayed two peaks with an isomer shift of 0.38 mms^{-1} and quadrupolar splitting of 0.69 mms^{-1}, which was corresponded to the iron glycolate. The iron glycolate was existed as the Fe (III). As shown in Figure 5(d), the Mössbauer spectrum shows just one double peaks without any other specific parameters characteristics. The isomer shift and quadrupolar splitting was 0.35 mms^{-1} and 0.71 mms^{-1} respectively, which corresponding to α-FeOOH as well. Furthermore, the line width reaches up to 0.54 mms^{-1}, which demonstrated the fabricated α-FeOOH was amorphous, and it was accorded with the XRD result. What's more, the results of Mössbauer spectra illustrated that both the iron glycolate and α-FeOOH were in high purity.[64–65] Furthermore, the inductively coupled plasma mass spectrometry characterization demonstrated that the content of iron in the α-FeOOH was 60%, which was close to theoretical 63% (calculated from chemical formula).

Optimization of experimental parameters for the reduction of 4-nitrophenol

The catalytic activities of all the prepared catalysts were evaluated through the reduction of 4-nitrophenol (Table 1), sequentially after optimizing the reaction temperature and the amount of the catalyst dosage (Table S1). The reaction procedure was described as follows: in a sealed tube, 1 mmol of 4-nitrophenol, 7 mg of catalyst, 2 mL solvent and a certain amount of hydrazine hydrate was added. Then the mixture solution was heated at 110 ºC in an oil bath. We firstly executed the reduction of 4-nitrophenol with excessive hydrazine hydrate in the ethanol. The reaction results showed that the reaction fully completed in 15 min and the TOF was up to 320 h^{-1} (entry 1). Encouraged by this anticipated result, we transferred this reaction to water, which is the "greenest" solvent. Meanwhile, the reduction of nitroaromatics in water is still a grand challenge, especially for the noble metal-free catalysts. When we used water as the solvent, the 4-nitrophenol can be completely converted into the 4-aminophenol in 45 min (entry 2). The dosage of the hydrazine hydrate was also investigated. Under the condition that the solvent was ethanol, the minimized amount of hydrazine hydrate could be 1.6 mmol (1.06 eq.), but for water it was 2.0 mmol (1.33 eq.) (entries 3-4). As the comparison, the iron glycolate, (precursor of α-FeOOH) and ferric chloride (raw material) and other iron-only catalysts were used as catalysts both in ethanol and water. For the iron glycolate, when the reaction was conducted under the same conditions of α-FeOOH, the conversion of 4-nitrophenol to the corresponding anilines was 89% (in ethanol) or 65% (in water), respectively (entries 5-6). The catalytic reaction results of ferric chloride were unsatisfactory as known reports, the conversion of 4-nitrophenol was only 10% and 2%, even the reaction time was extended to 180 min (entries 7-8). The widely reported Fe_3O_4, Fe_2O_3, and other FeOOH catalyst were also checked. The Fe_2O_3 and Fe_3O_4 were synthesized by calcining the iron glycolate (SI, Figure S2-3). The activity of these catalysts was less than the flowerlike amorphous α-FeOOH. The best conversion of all the reaction was 45%, even the reaction time was extended to 180 min (entries 9-12). Furthermore, the FeOOH with different morphologies and crystalline phases for this transformation were also investigated. The α-FeOOH that was synthesized as Lou reported[50] gave only 40 % (in ethanol) and 13% (in water) conversion (entries 13-14). The β-FeOOH and γ-FeOOH prepared by previous literatures reported[66-67] (Figure S9) displayed less than 45% conversion (entries 15-18). These results illustrated that the flowerlike amorphous α-FeOOH exhibited the best performance for the reduction of 4-nitrophenol.

Table 1. Optimization of experimental parameters for the reduction of 4-nitrophenol[a]

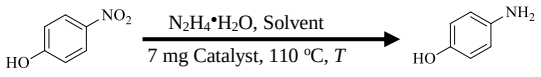

Entry	Catalyst	Solvent	N_2H_4 (mmol)	Time (min)	Conv. (%)[b]	TOF (h^{-1})
1	α-FeOOH	EtOH	3	15	100	320
2	α-FeOOH	H_2O	3	45	100	106
3	α-FeOOH	EtOH	1.6	15	100	320
4	α-FeOOH	H_2O	2	45	100	106
5	Iron glycolate	EtOH	1.6	15	89	180
6	Iron glycolate	H_2O	2	45	65	39
7	$FeCl_3$	EtOH	1.6	180	10	7
8	$FeCl_3$	H_2O	2	180	2	1.4
9	Fe_3O_4	EtOH	1.6	180	24	9
10	Fe_3O_4	H_2O	2	180	3	1.1
11	γ-Fe_2O_3	EtOH	1.6	180	45	16
12	γ-Fe_2O_3	H_2O	2	180	12	4
13[c]	α-FeOOH	EtOH	1.6	60	40	32
14[c]	α-FeOOH	H_2O	2	60	13	9
15[d]	β-FeOOH	EtOH	1.6	60	30	25
16[d]	β-FeOOH	H_2O	2	60	8	6
17[e]	γ-FeOOH	EtOH	1.6	60	45	36
18[e]	γ-FeOOH	H_2O	2	60	15	11

[a]The reaction was conducted under the condition of 1mmol 4-nitrophenol, 7 mg catalyst, 2 mL solvent, 110 °C; [b]The reaction was monited by TLC, conversion was detected by HPLC and GC-MS; [c]the α-FeOOH was fabricated as the ref. 50 reported; [d]the β-FeOOH was fabricated as the ref. 66 reported; [e] the γ-FeOOH was fabricated as the ref. 67 reported.

As shown in table S2, numerous of works have been reported for the reduction of nitroaromatics. Generally, when the noble metal was used as precursors, the fabricated catalysts have excellent catalytic activity. However, most of them required organic solvent and the dosages of hydrazine hydrate were much more than stoichiometric. Some works have attempted to use water as solvent, however, the results were seldom satisfactory (Table S2, entries 3, 5, 8). In this work, the amorphous α-FeOOH can completely catalyze 4-nitrophenol to aniline in a short time even when water was the solvent. To the best of our knowledge, compared with other iron-only catalysts that previous literatures reported, the catalytic activity of the amorphous α-FeOOH was the best one and the TOF was up to 106 h^{-1} with only 1.3 equivalent hydrazine hydrate. Stimulated by this result, a further research was conducted to explain this phenomenon. As shown in Figure 6(a), the SEM image of the catalyst that was used for two cycles demonstrates that after treating the catalyst under 110 °C, the surface of the catalyst produced large amounts of coral-like structure but it remains its amorphous state which benefits the reduction of nitroaromatics. The catalyst was further characterized by the nitrogen adsorption-desorption to analysis the specific surface area change.

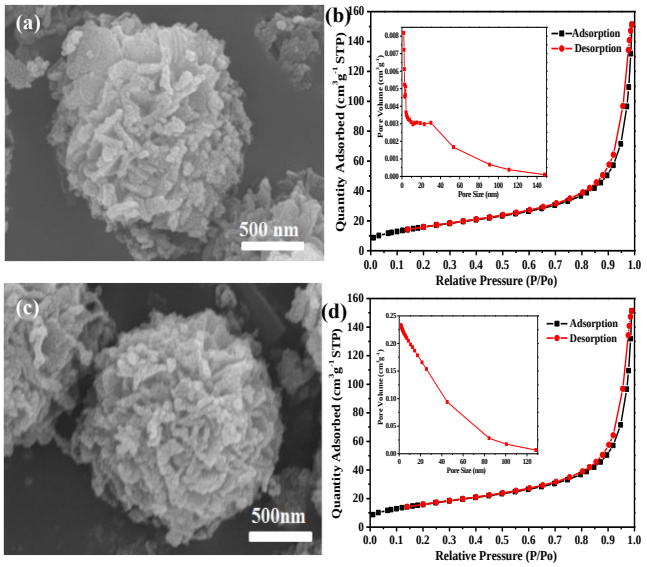

Figure 6. (a-b) SEM images and Nitrogen adsorption isotherms of the α-FeOOH after used for 2 times; (c-d) SEM and Nitrogen adsorption isotherms of the α-FeOOH after used 6 times.

The Figure 6(b) demonstrates that after the specific surface area of the catalyst decreased to 59 m^2g^{-1} used for two times, and the pores sizes of amorphous α-FeOOH turned to large pores with the size of 5-100 nm. Even after six cycles, the SEM image, nitrogen adsorption−desorption isotherms (Figure 6(c-d) and Figure S10), TEM images and EDS mapping (Figure S11) of the catalyst also indicated that the morphology and specific surface area of the catalyst did not display a distinct change.

In historic studies, the catalytic activity of iron catalyst for the hydrazine mediated reduction of nitroaromatics was reported to strongly depend on the surface area of the catalyst. In our forward research on the α-FeOOH, we found that the crystallinity was also a key factor. We obtained the pure amorphous α-FeOOH using the newly developed nanotechnology, then we synthesized a series of catalysts with different crystallinity by aging the amorphous α-FeOOH in 110 °C water for 5~25 hours. After testing their activity, we discovered that the catalytic activity vigorously depended on their crystallinity. As shown in the XRD spectrum (Figure 7(a)), the aged amorphous α-FeOOH was turned to α-Fe_2O_3 (JCPDS no.33-0664). The Figure 7(b) and Figure S12 illustrate the relationship between TOF and relative crystallinity according to the aged catalyst. It shows that the catalyst's activity drops with the crystallization of the

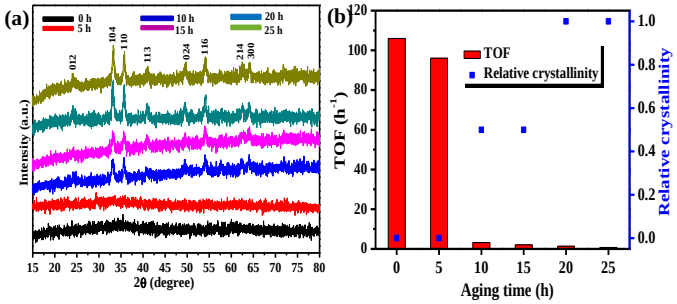

Figure 7. (a) XRD pattern of the catalyst after aging treatment; (b) the relationship between TOF and relative crystallinity of the aged catalyst.

α-FeOOH (the TOF decreased from 106 to 0.8 h^{-1}). On the contrary, the surface areas are less important for the FeOOH hierarchical nanoflower. We conducted the nitrogen adsorption isotherms characterization to obtain the specific surface area of the aged catalysts. As shows in Figure S13, the specific surface areas of the as-prepared and aged catalysts are 177 m^2g^{-1} (0 h), 70 m^2g^{-1} (5 h), 68 m^2g^{-1} (10 h), 71 m^2g^{-1} (15 h), 61 m^2g^{-1} (20 h), 66 m^2g^{-1} (25 h), respectively. The aged catalyst showed the same transformation with the recycled ones. Especially for the 5 h-aged and the 10 h-aged catalyst, their surface areas were almost the same, but their catalytic activity is quite different. The result proved that the crystallinity of the catalyst is the most significant factor for α-FeOOH.

The kinetics study of the catalytic transfer hydrogenation reaction system

As the most effective Fe-only catalyst for the hydrazine mediated reduction of nitroaromatics in water, the detailed kinetics study of the transformation for this catalytic system was conducted. The kinetics equation was established by dealing the relationship between concentration (c) and time (t), whereas the concentration was determined by measuring the gas (N_2) generation timely. The volume of gas was measured at 25 °C with a glass buret, then translated to the concentration of 4-nitrophenol. The detailed experiment was in the supporting information and the side reaction has been considered in the translation. The Figure 8 (a) shows the relation of α-FeOOH concentration with the nitro reduction rate at 90 °C. When the concentration of $N_2H_4{\cdot}H_2O$ and the concentration of 4-nitrophenol were identical, the rates were 0.0045 mol/(L·min), 0.0101 mol/(L·min) and 0.0123 mol/(L·min) and 0.0183 mol/(L·min) for 5, 10, 15, 20 mg catalyst respectively. Figure 8(b) indicates that the reaction is first-order for α-FeOOH. It can be seen in Figure 8(c) that the reaction rates from 80 °C to 110 °C are 0.0100 mol/(L·min), 0.0183 mol/(L·min), 0.0351 mol/(L·min) and 0.0768 mol/(L·min), respectively, when we use 20 mg catalyst. At 110 °C, a high yield of 4-aminophenol, namely 94%, was achieved within a short time of 8 min, this strongly supported that the amorphous α-FeOOH nanoflower exhibited excellent catalytic performance.

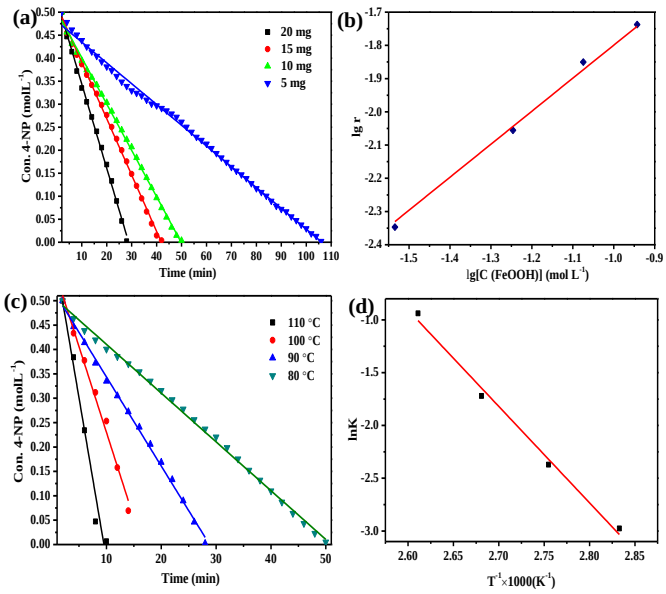

Figure 8. (a) Effect of α-FeOOH on the reduction of 4-nitrophenol by $N_2H_4{\cdot}H_2O$; (b) a plot of lg r vs lg(α-FeOOH) (α-FeOOH: 0.029~0.11 mol/L), where r means the reaction rate (mol/ (L·min)); (c) effect of reaction temperature on reduction of 4-nitrophenol by $N_2H_4{\cdot}H_2O$ over α-FeOOH catalyst; (d) Arrhenius plot for determination of the apparent activation energy E_a and the pre-exponential factor A (A=exp (22.8) mol/ (L·min)).

The linear relationship of Arrhenius plot is excellent (Figure 8 (d)), and according to this result, we calculated that the apparent activation energy of α-FeOOH catalyzed reduction of 4-nitrophenol by $N_2H_4{\cdot}H_2O$ is 75.9 kJ/mol (E_a=9.13×8.314 =75.9 kJ/mol), which is well agreed with the previous literature reported (E_a=75.7±1.0 kJ/mol)[34]. This reveals that the α-FeOOH nanoflower catalyzed reaction undergoes the identical chemical pathway with other iron-only catalysts, but the better activity lives in its special amorphous structure, which may offer a higher activation entropy for the reaction.[68]

In addition, the kinetics study of 4-nitrophenol and $N_2H_4{\cdot}H_2O$ for this reaction system were also investigated (Figure S14-S15). The plot of ln r versus ln (4-nitrophenol) (Figure S14 (b)) shows that the slope of -0.29 with a very good linearity of R^2 = 0.994, so the order of 4-nitrophenols (in this concentration range) can be deduced to be -0.29. Similarly, the plot of lg r versus lg [N_2H_4] (Figure S15 (b)) gives the result that the reaction order for the hydrazine in this system was 0.78. The kinetic study also reveals that the reaction occurs via the Langmuir-Hinshelwood mechanism, as both 4-nitrophenol and $N_2H_4{\cdot}H_2O$ are adsorbed on the α-FeOOH.

The scope of the reaction system

The utilization scope is a significant metric to evaluate the worth of a novel catalyst system. With that, a variety of structural diverse nitroaromatics have been applied to this optimized catalytic system as to check this catalyst and obtain the target aryl amines. As shown in table 2, no matter using ethanol or water as reaction solvent, all nitro compounds completed the reactions with 100% conversion in a short time. As previous works reported, by using noble metal-free catalyst in this transformation, azoxy, azo and hydrazo compounds were usually generated as the by-products[41]. In this reaction system, the nitroaromatics were reduced to the anticipated anilines with excellent conversion and chemoselectivity. The reaction results indicated that the flowerlike amorphous α-FeOOH was an excellent catalyst for this transformation. It is well known that halogen substituted anilines is a kind of key intermediates in pharmaceutical industry, such as chlorfluazuron and hexaflumuron. However, dehalogenation was usually occurred when the nitroaromatics were reduced. Due to this reason, some representative chloro-contained nitroarenes were applied to test this reaction system. The reaction results demonstrated that the dehalogenation was avoided under the reaction conditions for all these compounds (entries 3-6). Furthermore, this catalyst system was also used for reduction of other nitroarenes, including the derivatives that contained functional groups, such as alcohol, ester group, ether, amide and amino (entries 7-14). All of substrates were completely converted into the objective anilines and other functional groups kept without any change. Owing to amino-substituted heterocycles are important fine chemicals in industry, we investigated some nitro compounds contains heterocyclic ring moieties.

Table 2. Flowerlike amorphous α-FeOOH hierarchical supraparticles catalytic reduction of varieties nitroarenes with $N_2H_4{\cdot}H_2O$ in water and ethanol.

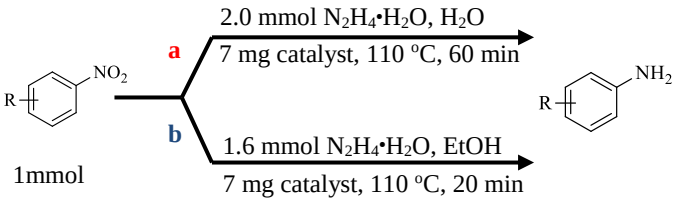

Entry	Substrate	Product	Conv. (%)	Sel. (%)
1	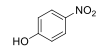	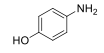	>99(>99)	>99(99)
2	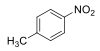	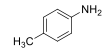	>99(>99)	>99(99)
3	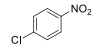	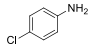	>99(>99)	>99(99)
4			>99(>99)	>99(99)
5	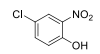	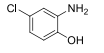	>99(>99)	>99(99)
6	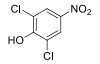	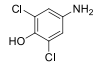	>99(>99)	>99(99)
7			>99(>99)	>99(99)
8	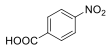	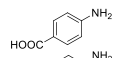	>99(>99)	>99(99)
9	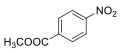	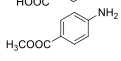	>99(>99)	>99(99)
10	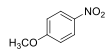	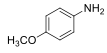	>99(>99)	>99(99)
11		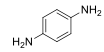	>99(>99)	>99(99)
12	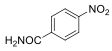	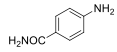	>99(>99)	>99(99)
13	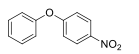	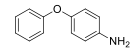	>99(>99)	>99(99)
14	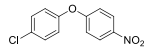	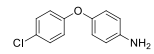	>99(>99)	>99(99)
15	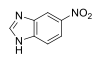	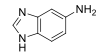	>99(>99)	>99(99)
16	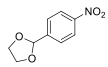	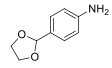	>99(>99)	>99(99)

[a]The reaction solvent was water, [b] the reaction solvent was ethanol. The reaction conversion and selectivity were detected by GC-MS.

As shows in entries 15-16, they have been transformed into corresponding heteroaromatic amines successfully with high yields. What's more, the heterocyclic rings were remained without any damage. Although many works have tried to use water as solvent for reduction of nitroaromatics, the reaction results were miserable. They demonstrated that the solubility of nitro compounds in water is another rate-determining step for this transformation apart from catalytic activity. In this work, even the nitroaromatics were not very well dissolved, this strictest obstacle can be overcome by the special morphology of flowerlike amorphous α-FeOOH hierarchical supraparticles[69], whose nano-porous surface offered the strong adsorb ability at the surfaces. By the way, in the hydrogen transfer reaction, the hydrazine hydrate can be facilely absorbed to the α-FeOOH

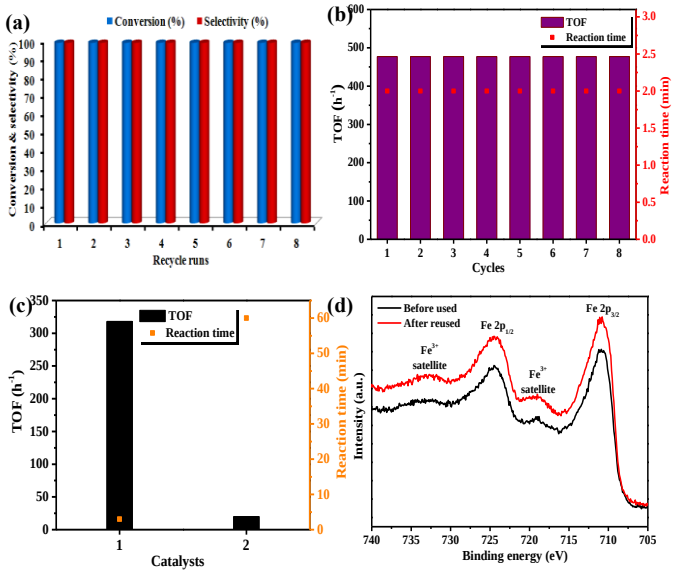

Figure 9. (a) Recycle test of the flowerlike amorphous α-FeOOH hierarchical supraparticles catalyst to reduction of 4-nitrophenol; (b) the TOF of the catalyst recycled with only 20% conversion; (c) the TOF of the aged catalysts recycled with only 20% conversion: (1) aged for 5 h; (2) aged for 10 h; (d) XPS Fe 2p region spectrum of the fresh and reused amorphous α-FeOOH.

and generate hydrogen species that can transfer to the substrates instantly. Due to the stability and recyclability are crucial metrics for a novel catalyst system, we explored the reusability of the amorphous α-FeOOH catalyst. The typical processing was conducted by adding 1 mmol of 4-nitrophenol, 7 mg of α-FeOOH and 2 mL water into a sealed tube. Then 2.0 mmol of hydrazine hydrate (125 mg, 80%) was dropped. The reactor was heated in an oil bath at 110 °C. After the reaction completed (monitored by TLC and GC-MS), the reactants were added into the vessel as the above mention. The catalyst system was reused for the next cycle without any cumbersome filtration process. This catalyst was conveniently reused for more than eight times for the reduction of 4- nitrophenol without any catalytic activity loss (Figure 9(a)). Furthermore, in order to further confirm the reaction results, the recycling ability of this catalytic system with only 20% conversion was also investigated and the detailed experiments were described in the supporting information. The results demonstrated that the reaction time for the 20% conversion was about 2 min. The TOF for the catalyst was up to 470 h^{-1}. Even used for 8 cycles, the 20% conversion can be obtained in 2 min (Figure 9(b)). Similarly, in order to further verify the effect of crystallinity on the catalytic properties, the TOF of the catalysts, which aged for 5 and 10 h, with only 20% conversion were also explored. The result obviously shows that as the crystallinity increased, the TOF of the catalyst decreased (Figure 9(c)) It was further confirmed the results of the Figure 7. Finally, the XRD, Mössbauer spectra, XPS, AFM and SEM (Figure S16-20) characterizations were also used to characterize the recycled catalyst. The results demonstrated that although the morphology of the catalyst was changed to coral-like structure, however, the chemistry properties, especially the amorphous crystallinity and chemical state of iron of the reused catalyst did not change. Furthermore, due to that the individual sizes of the catalyst supraparticles are not that small, so the transformation from amorphous state to crystalline is not that

easy. This helps the catalyst maintains its original activity for a sufficiently long period (more than 8 cycles).

As shown in Figure S21, based on the experimental results and available literatures data,[70] the mechanism for the reduction of nitroaromatics has been also proposed. Namely, the hydrazine hydrate was absorbed on the surface of the amorphous α-FeOOH then decomposed to generate hydrogen species. The substrates obtained hydrogen and gradually reduced to corresponding anilines. The general pathway for the reduction of nitroaromatics was following along the typical lines: Ar-NO_2→Ar-NO→Ar-NHOH→Ar-NH_2. The reasonable explanation of the higher catalytic activity than other iron-only catalyst is that the pure amorphous structure enhances the active entropy of the intermediates.

CONCLUSION

In summary, a pure flowerlike amorphous α-FeOOH hierarchical supraparticles have been facilely developed by in-situ hydrolysis of the self-assembled iron glycolate in water for the first time. This noble metal free catalyst has the highest activity among the Fe-only catalysts and exhibits good selectivity for the catalytic transfer hydrogenation of nitroarenes to the corresponding anilines by hydrated hydrazine in the greenest solvent-water. Following reaction, the amorphous crystal structure, special nanostructures and adsorption-desorption synergy offered the excellent activity. The kinetics study presents that the apparent active energy E_a is 75.9 kJ mol^{-1} and the reaction is a 1st order for Fe, which suggests that the active center may exist as the single Fe species.

ASSOCIATED CONTENT

Supporting Information

The Supporting Information is available free of charge on the ACS Publications website.

AUTHOR INFORMATION

Corresponding Author

E-mail: liangql@tsinghua.edu.cn

E-mail: sunhb@mail.neu.edu.cn

ORCID

Yongjian Ai: 0000-0003-3018-8027

Hong-bin Sun: 0000-0002-9007-4091

Qionglin Liang: 0000-0002-6750-038X

Notes

The authors declare no competing financial interest.

ACKNOWLEDGMENT

This work was financially supported by the National Natural Science Foundation of China (Nos. 81872835 and 21621003), the Ministry of Science and Technology (Nos. 2017YFC0906902 and 2017ZX09301032), and Macau Science and Technology Development Fund (129/2017/A3).

REFERENCES

(1) Bullock, R. M. Abundant metals give precious hydrogenation performance. *Science* **2013**, *342*, 1054−1055.

(2) Zhao, M. T.; Yuan, K.; Wang, Y.; Li, G.; Guo, J.; Gu, L.; Hu. W.; Zhao, H.; Tang, Z. Metal-organic frameworks as selectivity regulators for hydrogenation reactions. *Nature* **2016**, *539*, 76−80.

(3) Nie, Z.; Petukhova, A.; Kumacheva, E. Properties and emerging applications of self-assembled structures made from inorganic nanoparticles. *Nat. Nanotechnol.* **2010**, *5*, 15−25.

(4) Zhang, Y.; Guo, J.; Shi, L.; Zhu, Y.; Hou, K.; Zheng, Y.; Tang, Z. Tunable chiral metal organic frameworks toward visible light-driven asymmetric catalysis. *Sci. Adv.* **2017**; *3*, e1701162−e1701169.

(5) Fan, J. A.; Wu, C.; Bao, K.; Bao, J.; Bardhan, R.; Halas, N. J.; Manoharan, V. N.; Nordlander, P.; Shvets, G.; Capasso, F. Self-assembled plasmonic nanoparticle clusters. *Science* **2010**, *328*, 1135−1138.

(6) Love, J. C.; Estroff, L. A.; Kriebel, J. K.; Nuzzo, R. G.; Whitesides, G. M. Self-assembled monolayers of thiolates on metals as a form of nanotechnology. *Chem. Rev.* **2005**, *105*, 1103−1170.

(7) Wooh, S.; Huesmann, S.; Tahir, M. N.; Paven, M.; Wichmann, K.; Vollmer, D.; Tremel, W.; Papadopoulos, P.; Butt, H. Synthesis of mesoporous supraparticles on superamphiphobic surfaces. *Adv. Mater.* **2015**, *27*, 7338–7343.

(8) Zhong, L. S.; Hu, J. S.; Liang, H. P.; Cao, A. M.; Song, W. G.; Wan, L. J. Self-assembled 3D flowerlike iron oxide nanostructures and their application in water treatment. *Adv. Mater.* **2006**, *18*, 2426−2431.

(9) Hu, J. S.; Zhong, L. S.; Song, W. G.; Wan, L. J. Synthesis of hierarchically structured metal oxides and their application in heavy metal ion removal. *Adv. Mater.* **2008**, *20*, 2977−2982.

(10) Guo, J.; Yang, W.; Wang, C. Magnetic colloidal supraparticles: design, fabrication and biomedical applications. *Adv. Mater.* **2013**, *25*, 5196−214.

(11) Zhou, H.; Kim, J. P.; Bahng, J. H.; Kotov, N. A.; Lee, J. Self-assembly mechanism of spiky magnetoplasmonic supraparticles. *Adv. Funct. Mater.* **2014**, *24*, 1439−1448.

(12) Xia, Y. S.; Tang, Z. Y. Monodisperse hollow supraparticles via selective oxidation. *Adv. Funct. Mater*. **2012**, *22*, 2585–2593.

(13) Xia, Y.; Nguyen, T. D.; Yang, M.; Lee, B.; Santos, A.; Podsiadlo, P.; Tang, Z.; Glotzer, S. C.; Kotov, N. A. Self-assembly of self-limiting monodisperse supraparticles from polydisperse nanoparticles. *Nat. Nanotechnol.* **2011**, *6*, 580−587.

(14) Li, Y.; Shi, J. Hollow-structured mesoporous materials: chemical synthesis, functionalization and applications. *Adv. Mater.* **2014**, *26*, 3176−205.

(15) Whitesides, G. M.; Grzybowski, B. Self-assembly at all scales. *Science* **2002**, *295*, 2418−2421.

(16) Ling, D.; Lee, N.; Hyeon, T. Chemical synthesis and assembly of uniformly sized iron oxide nanoparticles for medical applications. *Acc. Chem. Res.* **2015**, *48*, 1276−1285.

(17) Byun, S.; Song, Y.; Kim, B. M. Heterogenized bimetallic Pd-Pt-Fe_3O_4 nanoflakes as extremely robust, magnetically recyclable catalysts for chemoselective nitroarene reduction. *ACS Appl. Mater. Inter.* **2016**, *8*, 14637–14647.

(18) Enthaler, S.; Junge, K.; Beller, M. Sustainable metal catalysis with iron: from rust to a rising star. *Angew. Chem. Int. Ed.* **2008**, *47*, 3317 −3321.

(19) Bauer, I.; Knolker, H. J. Iron catalysis in organic synthesis. *Chem. Rev*. **2015**, *115*, 3170−3187.

(20) Wang, C.; Ciganda, R.; Salmon, L.; Gregurec, D.; Irigoyen, J.; Moya, S.; Ruiz, J.; Astruc, D. Highly efficient transition metal nanoparticle catalysts in aqueous solutions. *Angew. Chem. Int. Ed.* **2016**, *55*, 3091−3095.

(21) Ai, Y.; He, M.; Lv, Q.; Liu, L.; Sun, H.; Ding, M.; Liang, Q. 3D porous carbon framework stabilized ultra−uniform nano γ-Fe_2O_3: a useful catalyst system. *Chem. Asian. J*. **2018**, *13*, 89–98.

(22) Li, Y. Y.; Yu, S. L.; Shen, W. Y.; Gao, J. X. Iron-, cobalt-, and nickel-catalyzed asymmetric transfer hydrogenation and asymmetric hydrogenation of ketones. *Acc. Chem. Res.* **2015**, *48*, 2587−2598.

(23) Huang, H. G., Tang, M. W.; Wang, X. G.; Zhang, M. ; Guo, S. Q.; Zou, X. J.; Lu, X. G. Synthesis of mesoporous gamma-alumina-supported Co-based catalysts and their catalytic performance for chemoselective reduction of nitroarenes. *ACS Appl. Mater. Inter.* **2018**, *10*, 5413–5428.

(24) Ai, Y.; Hu, Z.; Shao, Z.; Qi, L.; Liu, L.; Zhou, J.; Sun, H.; Liang, Q. Egg-like magnetically immobilized nanospheres: a long-lived catalyst model for the hydrogen transfer reaction in a continuous-flow reactor. *Nano Res.* **2018**, *11*, 287−299.

(25) Sorribes, I.; Wienhofer, G.; Vicent, C.; Junge, K.; Llusar, R.; Beller, M. Chemoselective transfer hydrogenation to nitroarenes mediated by cubane-type Mo_3S_4 cluster catalysts. *Angew. Chem. Int. Ed.* **2012**, *51*, 7794−7798.

(26) Zhou, J.; Li, Y.; Sun, H. B.; Tang, Z.; Qi, L.; Liu, L.; Ai, Y.; Li, S.; Shao, Z.; Liang, Q. Porous silica-encapsulated and magnetically recoverable Rh NPs: a highly efficient, stable and green catalyst for catalytic transfer hydrogenation with “slow-release” of stoichiometric

hydrazine in water. *Green Chem.* **2017**, *19*, 3400−3407.

(27) Das, V. K.; Mazhar, S.; Gregor, l.; Stein, B.; Morgan, D.; Maciulis, N. A.; Pink, M.; Losovyj, Y.; Bronstein, L. M. Graphene derivative in magnetically recoverable catalyst determines catalytic properties in transfer hydrogenation of nitroarenes to anilines with 2-propanol. *ACS Appl. Mater. Inter.* **2018**, *10*, 25, 21356−21364.

(28) Schwob, T.; Kempe, R. A reusable Co catalyst for the selective hydrogenation of functionalized nitroarenes and the direct synthesis of imines and benzimidazoles from nitroarenes and aldehydes. *Angew. Chem. Int. Ed.* **2016**, *55*, 15175−15179.

(29) Ai, Y.; Liu, L.; Jing, K.; Qi, L.; Fan, Z.; Zhou, J.; Sun, H.; Shao, Z.; Liang, Q. Noncovalently functionalized carbon nanotubes immobilized Fe-Bi bimetallic oxides as a heterogeneous nanocatalyst for reduction of nitroaromatics. *Nano-Struct. Nano-Objects.* **2017**, *10*, 116−124.

(30) Corma, A.; Serna, P. Chemoselective hydrogenation of nitro compounds with supported gold catalysts. *Science* **2006**, *313*, 332−334.

(31) Zhang, S.; Chang, C. R.; Huang, Z. Q.; Li, J.; Wu, Z.; Ma, Y.; Zhang, Z.; Wang, Y.; Qu, Y. High catalytic activity and chemoselectivity of sub-nanometric Pd clusters on porous nanorods of CeO_2 for hydrogenation of nitroarenes. *J. Am. Chem. Soc.* **2016**, *138*, 2629−2637.

(32) Westerhaus, F. A.; Jagadeesh, R. V.; Wienhofer, G.; Pohl, M. M.; Radnik, J.; Surkus, A. E.; Rabeah, J.; Junge, K.; Junge, H.; Nielsen, M.; Bruckner, A.; Beller, M. Heterogenized cobalt oxide catalysts for nitroarene reduction by pyrolysis of molecularly defined complexes. *Nat. Chem.* **2013**, *5*, 537−543.

(33) Sun, H.; Ai, Y.; Li, D.; Tang, Z.; Shao, Z.; Liang, Q. Bismuth iron oxide nanocomposite supported on graphene oxides as the high efficient, stable and reusable catalysts for the reduction of nitroarenes under continuous flow conditions. *Chem. Eng. J.* **2017**, *314*, 328−335.

(34) Lauwiner, M.; Rys, P.; Wissmann, J. Reduction of aromatic nitro compounds with hydrazine hydrate in the presence of an iron oxide hydroxide catalyst. I. the reduction of monosubstituted nitrobenzenes with hydrazine hydrate in the presence of ferrihydrite. *Appl. Catal. A-Gen.* **1998**, *172*, 141−148.

(35) Benz, M.; van der Kraan, A. M.; Prins, R. Reduction of aromatic nitrocompounds with hydrazine hydrate in the presence of an iron oxide hydroxide catalyst: II. activity, X-ray diffraction and Mössbauer study of the iron oxide hydroxide catalyst. *Appl. Catal. A-Gen.* **1998,** *172*, 149−157.

(36) Lauwiner, M.; Roth, R.; Rys, P. Reduction of aromatic nitro compounds with hydrazine hydrate in the presence of an iron oxide/hydroxide catalyst. III. the selective reduction of nitro groups in aromatic azo compounds *Appl. Catal. A-Gen.* **1999**, *177*, 9−14.

(37) Benz, M.; Prins, R. Reduction of aromatic nitro compounds with hydrazine hydrate in the presence of an iron oxide/hydroxide catalyst. III. The selective reduction of nitro groups in aromatic azo compounds. *Appl. Catal. A-Gen.* **1999**, *183*, 325−333.

(38) Cantillo, D.; Baghbanzadeh, M.; Kappe, C. O. In situ generated iron oxide nanocrystals as efficient and selective catalysts for the reduction of nitroarenes using a continuous flow method. *Angew. Chem. Int. Ed.* **2012**, *51*, 10190−10193.

(39) Shi, Q.; Lu, R.; Jin, K.; Zhang, Z.; Zhao, D. Simple and eco-friendly reduction of nitroarenes to the corresponding aromatic amines using polymer-supported hydrazine hydrate over iron oxide hydroxide catalyst. *Green Chem.* **2006**, *8*, 868−870.

(40) Wienhofer, G.; Sorribes, I.; Boddien, A.; Westerhaus, F.; Junge, K.; Junge, H.; Llusar, R.; Beller, M. General and selective iron-catalyzed transfer hydrogenation of nitroarenes without base. *J. Am. Chem. Soc.* **2011**, *133*, 12875−12879.

(41) Jagadeesh, R. V.; Surkus, A. E.; Junge, H.; Pohl, M. M.; Radnik, J.; Rabeah, J.; Huan, H.; Schuenemann, V.; Brueckner, A.; Beller, M. Nanoscale Fe_2O_3-based catalysts for selective hydrogenation of nitroarenes to anilines. *Science* **2013**, *342*, 1073−1076.

(42) Jagadeesh, R. V.; Stemmler, T.; Surkus, A. E.; Junge, H.; Junge, K.; Beller, M. Hydrogenation using iron oxidebased nanocatalysts for the synthesis of amines. *Nat. Protoc.* **2015**, *10*, 548−557.

(43) Papadas, I. T.; Fountoulaki, S.; Lykakis, I. N.; Armatas, G. S. Controllable synthesis of mesoporous iron oxide nanoparticle assemblies for chemoselective catalytic reduction of nitroarenes. *Chem. Eur. J.* **2016**, *22*, 4600−4607.

(44) Tian, M.; Cui, X.; Yuan, M.; Yang, J.; Ma, J.; Dong, Z. Efficient chemoselective hydrogenation of halogenated nitrobenzenes over an easily prepared γ-Fe_2O_3-modified mesoporous carbon catalyst. *Green Chem.* **2017**, *19*, 1548−1554.

(45) Gu, X.; Sun, Z.; Wu, S.; Qi, W.; Wang, H.; Xu, X.; Su, D. Surfactant-free hydrothermal synthesis of sub-10 nm γ-Fe_2O_3-polymer porous composites with high catalytic activity for reduction of nitroarenes. *Chem. Commun.* **2013**, *49*, 10088−10090.

(46) Cantillo, D.; Moghaddam, M. M.; Kappe, C. O. Hydrazine-mediated reduction of nitro and azide functionalities catalyzed by highly active and reusable magnetic iron oxide nanocrystals. *J. Org. Chem.* **2013**, *78*, 4530−4542.

(47) Moghaddam, M. M.; Pieber, B.; Glasnov, T.; Kappe, C. O. Immobilized iron oxide nanoparticles as stable and reusable catalysts for hydrazine-mediated nitro reductions in continuous flow. *ChemSusChem* **2014**, *7*, 3122−3131.

(48) Zhu, K. L.; Shaver, M. P.; Thomas, S. P. Chemoselective nitro reduction and hydroamination using a single iron catalyst. *Chem. Sci*. **2016**, *7*, 3031–3035.

(49) She, W.; Qi, T.; Q. J.; Cui, M. X.; Yan, P. F.; Ng, S. W.; Li, W. Z.; Li, G. M. High catalytic performance of a CeO_2-supported Ni catalyst for hydrogenation of nitroarenes, fabricated via coordination-assisted strategy. *ACS Appl. Mater. Inter*. **2018**, *10*, 14698–14707.

(50) Wang, B.; Wu, H.; Yu, L.; Xu, R.; Lim, T. T.; Lou, X. W. Template-free formation of uniform urchin-like α-FeOOH hollow spheres with superior capability for water treatment. *Adv. Mater.* **2012**, *24*, 1111−1116.

(51) Hou, X.; Huang, X.; Jia, F.; Ai, Z.; Zhao, J.; Zhang, L. Hydroxylamine promoted goethite surface fenton degradation of organic pollutants. *Environ. Sci. Technol*. **2017**, *51*, 5118−5126.

(52) Yang, S.; Sun, Y.; Chen, L.; Hernandez, Y.; Feng, X.; Mullen, K. Porous iron oxide ribbons grown on graphene for high-performance lithium storage. *Sci. Rep.* **2012**, *2*, 427−434.

(53) Tong, G.; Liu, Y.; Wu, T.; Ye, Y.; Tong, C. High-quality elliptical iron glycolate nanosheets: selective synthesis and chemical conversion into Fe_xO_y nanorings, porous nanosheets, and nanochains with enhanced visible-light photocatalytic activity. *Nanoscale* **2015**, *7*, 16493−16503.

(54) Shen, J.; Zhu, J.; Kong, Y.; Li, T.; Chen, Z. Synthesized heterogeneous fenton-like goethite (FeOOH) catalyst for degradation of *p*-chloronitrobenzene. *Water. Sci. Technol.* **2013**, *68*, 1614−1621.

(55) Liu, J.; Zheng, M.; Shi, X.; Zeng, H.; Xia, H. Amorphous FeOOH quantum dots assembled mesoporous film anchored on graphene nanosheets with superior electrochemical performance for supercapacitors. *Adv. Funct. Mater.* **2016**, *26*, 919−930.

(56) Li, Z. C.; Guan, M. Y.; Lou, Z. S.; Shang, T. M. Facile hydrothermal synthesis and electrochemical properties of flowerlike α−FeOOH. *Micro. Nano. Letter.* **2012**, *7*, 33−36.

(57) Chen, H. F.; Wei, G. D.; Han, X.; Li, S.; Wang, P. P.; Chubik, M.; Gromov, A.; Wang, Z. P.; Han, W. Large-scale synthesis of hierarchical alpha-FeOOH flowers by ultrasonic-assisted hydrothermal route. *J. Mater. Sci. Mater. El.* **2010**, *22*, 252−259.

(58) Ulhaq, I.; Haider, F. Synthesis and characterization of uniform fine particles of iron (III) hydroxide/oxide. *J. Chin. Chem. Soc.* **2010**, *57*, 174−179.

(59) Goldsmith, B. R.; Peters, B.; Johnson, J. K.; Gates, B. C.; Scott, S. L. Beyond ordered materials: understanding catalytic sites on amorphous solids. *ACS Catal*. **2017**, *7*, 7543−7557.

(60) Milone, C.; Ingoglia, R.; Schipilliti, L.; Crisafulli, C.; Neri, G.; Galvagno, S. Selective hydrogenation of α, β-unsaturated ketone to α, β-unsaturated alcohol on gold−supported iron oxide catalysts: role of the support. *J. Catal.* **2005**, *236*, 80−90.

(61) Rahimi, M.; Zinadini, S.; Zinatizadeh, A. A.; Vatanpour, V.; Rajabi, L.; Rahimi, Z. Hydrophilic goethite nanoparticle as a novel antifouling agent in fabrication of nanocomposite polyethersulfone membrane. *J. Appl. Polym. Sci.* **2016**, *133*, 43592−43605.

(62) Defaria, D. L. A.; Silva, S. V.; Deoliveira, M. T. Raman microspectroscopy of some iron oxides and oxyhydroxides. *J. Raman. Spectrosc.* **1997**, *28*, 873−878.

(63) Cwiertny, D. M.; Hunter, G. J.; Pettibone, J. M.; Scherer, M. M.; Grassian, V. H. Surface chemistry and dissolution of α-FeOOH nanorods and microrods: environmental implications of size-dependent interactions with oxalate. *J. Phys. Chem. C.* **2009**, *113*, 2175−2186.

(64) Forsyth, J. B.; Hedley, I. G.; Johnson, C. E. The magnetic structure and hyperfine field of goethite (α−FeOOH). *J. Phys. C-Solid. State. Phys.* **1968**, *1*,179−188.

(65) Johnson, C. E. Antiferromagnetism of γ-FeOOH: a Mössbauer effect study. *J. Phys. C- Solid. State. Phys.* **1969**, *2*, 1996−2002.

(66) Wang, X.; Chen, X. Y.; Gao, L. S.; Zheng, H. G.; Ji, M. R.; Tang, C. M.; Shen, T.; Zhang, Z. D. Synthesis of β-FeOOH and α-Fe_2O_3 nanorods and electrochemical properties of β-FeOOH. *J. Mater. Chem.* **2004**, *14*, 905–907.

(67) Rahimi, A.; Moattari, R.; Rajabi, R.; Derakhshan, A. A.; Keyhani, M. Iron oxide/hydroxide (α, γ-FeOOH) nanoparticles as high potential adsorbents for lead removal from polluted aquatic media. *J. Ind. Eng. Chem.* **2015**, *23*, 33–43.

(68) Zhong, R. Y.; Sun, K. Q.; Hong, Y. C.; Xu, B. Q. Impacts of organic stabilizers on catalysis of Au nanoparticles from colloidal preparation. *ACS Catal*. **2014**, *4*, 3982−3993.

(69) Zhou, L.; Xiu, F.; Qiu, M.; Xia, S.; Yu, L. The adsorption and dissociation of water molecule on goethite (010) surface: a DFT approach. *Appl. Surf. Sci.* **2017**, *392*, 760−767.

(70) Zhang, C.; Lu, J.; Li, M.; Wang, Y.; Zhang, Z.; Chen, H.; Wang, F. Transfer hydrogenation of nitroarenes with hydrazine at near-room temperature catalysed by a MoO_2 catalyst. *Green Chem.* **2016**, *18*, 2435−2442.

TOC

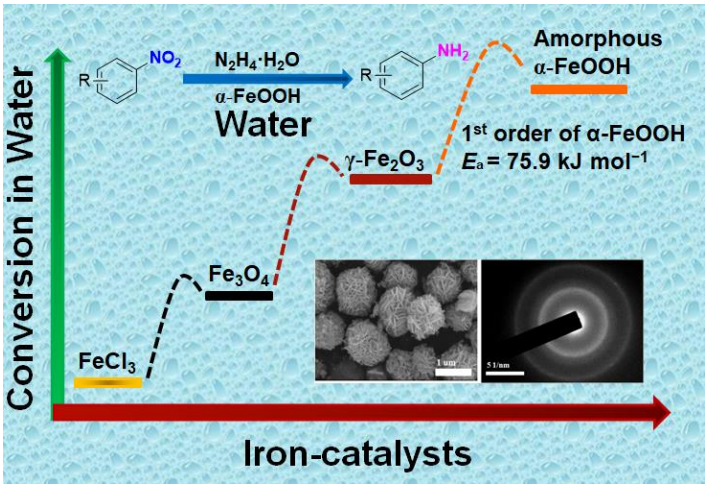

we developed a scalable hydrolysis method for synthesizing flowerlike amorphous α-FeOOH hierarchical supraparticles. Compared with other iron-only catalysts, this amorphous α-FeOOH hierarchical supraparticles catalyst exhibits the best performance in the catalytic reduction of nitro aromatics in water. Following reaction, the amorphous crystal structure, special nanostructures and adsorption-desorption synergy offered the excellent activity. The reduction of 4-nitrophenol is first-order for α-FeOOH and the apparent active energy E_a is 75.9 kJ mol^{-1}.